Optimization Design of High-Dimensional Parameters MIMO Antenna in Semantic-Based Mobile Applications

Qianqian Li, School of Electronics and Communications, Guangdong Mechanical and Electronical Polytechnic, China*

Jian Dong, School of Electronic Information, Central South University, China

ABSTRACT

To ensure the quality of semantic communication, an optimization scheme for multiple-input and multiple-output (MIMO) antenna design using in semantic-based mobile is proposed and verified. The scheme is based on a modified algorithm MOEA/D-BH, which integrates the black-hole (BH) algorithm into multi-objective EA based on decomposition (MOEA/D). By introducing controllable absorption distance and neighborhood learning mechanism, MOEA/D-BH can deal with high-dimension parameters well in a multi-objective optimization problem. Thus, in a limited design space, a satisfied antenna can be optimized by proposed scheme efficiently. This can be a feasible candidate scheme for MIMO antenna design. A single-band and dual-band MIMO antenna, which are applied for semantic-based mobile system, are optimized by proposed scheme sharing the same model. Both the data of simulation and measurement show good electrical and MIMO performances in the working frequency band. Thus not only the performance of the semantic communication definitely improved, but also it provides useful exploration for the development of intelligent semantic mobile systems.

KEYWORDS

BH Algorithm, High-Dimension Parameters Optimization, MIMO Antenna, MOEA/D, Multi-Objective, Semantic Communication

INTRODUCTION

Because of their intelligence and automation, evolutionary algorithms (EAs) have extensive use in a variety of fields (Lv et al., 2022; Behera et al., 2023; Rahman et al., 2022; Fatemidokht et al., 2021; Singh et al., 2024; Geng et al., 2022). Their effectiveness has also been validated in some antenna-design scenarios (Srivastava et al., 2022; Dong et al., 2018; Kaur & Sivia, 2022; Nouri et al., 2021). As the influence of semantic research increases (Hu et al., 2022; Nhi et al., 2022; Capuano et al., 2022), it is essential to design high-performance multiple-input and multiple-output (MIMO) antennas for semantic-based mobile phones to ensure quality semantic communication. Because those semantic-based mobiles are always becoming thinner while more components need to fit in them, there is limited space to distribute antenna elements, and the isolation of multiple antennas is greatly affected. While traditional MIMO antenna design depends mainly on the prior experience of the

designer, some techniques (Zhang et al., 2010; Wang & Du, 2015; Zou et al., 2019; Wen et al., 2018; Li et al., 2022) are always used. These methods, however, are difficult to apply on semantic-based mobile MIMO antenna design and the design complexity will increase greatly, especially when there are multiple design objectives and limitations. Thus, EAs are considered as an alternative scheme for semantic-based mobile MIMO antenna design.

Those designs are often related to high-dimensional parameters and multi-objective optimization problems (MOPs). With a distinctive multi-objective decomposition operation, multi-objective EA based on decomposition (MOEA/D) (Zhang & Li, 2007) shows good optimization quality in those similar multi-objective algorithms. One drawback of MOEA/D is that its original evolution strategy cannot handle MOPs with complicated Pareto sets well (Li & Zhang, 2009). Thus, an appropriate strategy should replace the original one to improve its performance (Li & Zhang, 2009; Li et al., 2020a) and make MOEA/D more suitable for high-dimensional parameter MIMO antennas in semantic-based mobile applications.

In this paper, the black-hole (BH) algorithm (Hatamlou, 2013) is modified and then integrated into MOEA/D to design semantic-based mobile MIMO antennas. In MOEA/D-BH, a controllable absorption distance is introduced to strengthen its global-optimization ability and a neighborhood learning mechanism can adjust its local searching capability well. Thus, it can provide a required design with accelerated convergence speed for high-dimension parameters. As for the antenna-structure optimization, discrete fragment patches are used as the optimization design parameters (Han et al., 2015). Two MIMO antennas, which are working under 5G/sub-6 GHz bands, are optimized to prove the effectiveness of the proposed scheme. Moreover, an eight-port MIMO antenna is configured based on the above design. All antennas are fabricated and measured to verify their performance and its feasibility in semantic-based MIMO antenna design.

IMPROVED ALGORITHM: MOEA/D-BH

MOEA/D-BH

Multiple objectives are well addressed by an intelligent decomposition strategy in MOEA/D, and BH can provide a satisfactory evolutionary process for the problem. MOEA/D-BH is proposed based on the above two features.

N is the population size, and each star i represents a subproblem in MOEA/D-BH. N weight vectors $\lambda^1, \lambda^2, ..., \lambda^N$ are generated by the Tchebycheff approach (Miettinen, 1999), and each weight vector λ^i corresponds to a subproblem i. Function $g(\mathbf{x}_i \mid \lambda^i)$ can evaluate the performance of subproblem i, where $\mathbf{x}_i$ is its position. Eventually, the optimized results are distributed in the Pareto front (PF) from λ^1 to λ^N uniformly. In the process of optimization, a black hole is responsible for absorbing surrounding stars and improving the positions of other stars. If a star falls within the radius of a black hole R, the star will be absorbed and occupy a new position; otherwise, its position will be optimized further. Thus, it is important to define the distance between a star and the black hole. For multi-objective optimization, multiple black holes are used to avoid falling into local optimum. In this paper, we consider bi-objective optimization, and so on for other cases.

For bi-objective optimization, two black holes are defined. One is the best star among weight vectors $\lambda^1, \lambda^2, ..., \lambda^{N/2}$, and the other one is recommended by the remaining stars. Weight vectors λ^1 to λ^N are distributed evenly, and then the two black holes can be beneficial for the two objectives, respectively. The radius of each black hole j is calculated as follows:

$$R_j = \frac{g_{BH}^j\left(\mathbf{x}_{BH}^j \mid \lambda^{j\_BH}\right)}{\sum_{i=1}^N g(\mathbf{x}_i \mid \lambda^i)} \quad j = 1, 2 \tag{1}$$

where $\mathbf{x}_{BH}^{j}$, λ^{j-BH} , and g_{BH}^{j} are the position, weight vector, and fitness value of black hole j. Then a controllable absorption distance formula for star i is proposed as follows:

$$d(i) = \frac{\omega * g_{BH}^1 * g_{BH}^2 * \mid g(\mathbf{x}_i \mid \lambda^i) - g_{BH}^j \mid}{\sum_{i=1}^{N} g(\mathbf{x}_i \mid \lambda^i)} \tag{2}$$
$$i \le N\big/2, j = 1; i > N\big/2, j = 2$$

where $\omega \in [0.1, 0.5]$ is absorptivity. For star i, if $d(i)$ is less than the radius of its corresponding black hole, its position will be updated by a neighborhood learning mechanism:

$$\mathbf{x}_i' = \mathbf{x}_{\min} + \mathbf{x}_{\max} - \mathbf{x}_i \tag{3}$$

where $\mathbf{x}_{\min}$ and $\mathbf{x}_{\max}$ are the minimum and maximum value in neighbors of star i. If not, its position will be updated as:

$$\mathbf{x}_i' = \mathbf{x}_i + \sum_{j=1}^{2} \frac{rand * (\mathbf{x}_{BH}^j - \mathbf{x}_i)}{j^2} \quad i \le N\big/2$$
$$\mathbf{x}_i' = \mathbf{x}_i + \sum_{j=1}^{2} \frac{rand * (\mathbf{x}_{BH}^j - \mathbf{x}_i)}{(j-3)^2} \quad i > N\big/2 \tag{4}$$

The following are the steps of MOEA/D-BH:

Step 1: Initialization
- ◦ Step 1.1: Define the position of *N* stars at random or by a particular problem;
- ◦ Step 1.2: Generate *N* weight vectors and contribute to *N* subproblems;
- ◦ Step 1.3: Find *T* neighbors for each star *i*;
- ◦ Step 1.4: Evaluate the objective function $g(\mathbf{x}_i \mid \lambda^i)$ of each star *i* and find two black holes;
- ◦ Step 1.5: Define an external population (EP) to put nondominated solutions obtained at present and set $EP = \varnothing$.

Step 2: Update
- ◦ Step 2.1: Judge whether a star is absorbed or not, and update the location of each star as in Formulas (3) and (4);
- ◦ Step 2.2: Reevaluate the objective function $g(\mathbf{x}_i \mid \lambda^i)$ of each star *i* and reset two black holes;
- ◦ Step 2.3: Update EP;
- ◦ Step 2.4: If termination criteria are reached, Step 3 will be implemented; otherwise, continue to do Step 2.

Step 3: Return EP

Discussion

For a MOP, if a set of representative solutions distributed along the PF is obtained by a multi-objective algorithm, it can be seen as an excellent algorithm (Marler and Arora, 2004). In target space, there is no special relation between adjacent results. With two black holes in MOEA/D-BH, all stars are

guided into the different segment of PF separately and two optimization objectives can be taken into account without bias. Then the obtained results can distribute as uniformly in the PF as possible.

For BH, a star that is within its event horizon will be absorbed by the black hole. Other unabsorbed stars are guided to move forward by the black hole. If the range of the event horizon (i.e., absorption distance) cannot be defined well, the population diversity of BH will be reduced greatly and the optimization process will fall into local optimization easily. In MOEA/D-BH, a controllable absorption distance is proposed to improve this. A random absorptivity ω can control the absorption distance and the number of absorbed stars further. The smaller the ω, the more stars can be absorbed and more new stars can be generated. However, if ω is too small, the randomness of the algorithm will increase greatly and those satisfied solutions are easily missed. Thus, ω is from 0.1 to 0.5 in this paper. With such a controllable absorption mechanism, the population diversity can be increased effectively. Therefore, it is more suitable for high-dimensional parameter optimization.

Moreover, those absorbed stars, which are reset by the neighborhood learning mechanism, can provide more abundant candidate solutions. Then better stars are more likely to obtain. For those unabsorbed stars, both black holes provide beneficial information for them. A star will get more information from its corresponding black hole and less information from another black hole; thus, these stars are emphasizing on different objectives and meet the requirements cooperatively. Hence, the global search ability is enhanced and the convergence speed is accelerated. Eventually, MOEA/D-BH can better realize the design of semantic-based mobile MIMO antennas.

MIMO ANTENNA DESIGN

In this section, two two-port MIMO antennas are optimized and an eight-port MIMO antenna is further designed. The performance of the obtained MIMO antennas and the feasibility of the proposed scheme are validated by both the simulated and the measured results. The geometry of the MIMO antenna model is depicted in Fig. 1, which will be optimized by our scheme. The system circuit board is a FR-4 $150 \times 75 \times 0.8 \ mm^3$ typically matching with a 5.8-inch smartphone. On the back of the substrate, a system ground plane ($134 \times 75 \ mm^2$) is printed. Two rectangular clearance areas of size $8 \times 75 \ mm^2$ are prepared for 2/3/4G antennas. On the two long edges of the system substrate, two small FR-4 substrates are placed vertically and the dimension of both is $134 \times 0.8 \times 6 \ mm^3$. Antennas 1 and 2, whose design space is limited to the dotted box of size $18 \times 6 \ mm^2$ on a long edge, will be obtained by the proposed multi-objective optimization scheme. The two antennas are symmetrically designed, and the distance between them is 12 mm. Each antenna is fed with a T-shaped feedline. The antenna element of an optimized MIMO antenna is used in an eight-port MIMO antenna, and

Figure 1. Geometry of the MIMO Antenna (Ant) Model
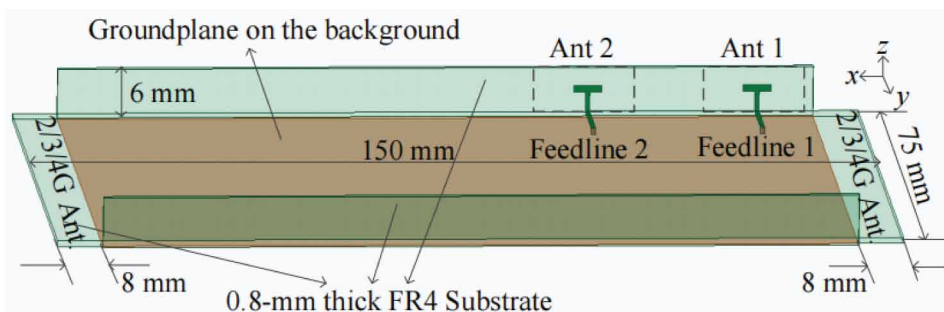
its performance is also studied. The simulation operating environment is equipped with 64-bit operating systems, 128GB RAM, and an Intel 3.50 GHz i9 processor.

Single-Band MIMO Antenna Design

There are many problems in designing semantic-based mobile MIMO antennas, especially in a limited design space. Here, a single-band MIMO antenna, which can cover long-term evolution (LTE) Band 46 (5.150–5.925 GHz), is designed automatically by improved MOEA/D-BH and fragment structure. The available space of Antennas 1 and 2 is predefined and shown in Fig. 2. The dotted box is discretized into 18×6 small elements (i.e., 108 parameters to be optimized), and each element is 1×1 mm^2. Then MOEA/D-BH is used to optimize it, and its evaluation function is expressed as follows:

$$f_1(\mathbf{x}) = \max(6 - \min_{s \in [s_1, s_2]} | S_{11} |, 0)$$
$$f_2(\mathbf{x}) = \max(15 - \min_{s \in [s_1, s_2]} | S_{12} |, 0)$$

(5)

where $[s_1, s_2]$ defines the operation band of the MIMO antenna. The lowest value of S_{11} and S_{12} is guaranteed to be greater than 6 dB and 15 dB by $f_1(\mathbf{x})$ and $f_2(\mathbf{x})$, respectively. Fig. 2 presents an antenna structure selected from PF after multiple iterations by MOEA/D-BH.

The antenna shown in Fig. 2 is simulated and measured, and its corresponding S-parameters are exhibited in Fig. 3. The results of measured S-parameters are consistent with the simulation data. It can be observed that the antenna operates at 4.96–6.06 GHz, which can cover LTE Band 46. And in the whole band, its isolation also exceeds 20 dB. Good S-parameter characteristics verify the feasibility of the optimized MIMO antenna.

As mentioned above, a successful multi-objective optimization can get a set of representations distributed uniformly in the PF. The advancing trails of some representative stars of antenna optimization by MOEA/D-BH are depicted in Fig. 4. Initially, those stars have disorderly arrangement in the design space. They then approach the PF gradually by iteration optimization. Eventually, the obtained Pareto optimal solutions distribute along the PF discretely. In fact, if desired solutions do not appear at the end of the iteration, the final results can be used to redefine the initial design space and effectively help follow-up optimization. This evolution process shows the applicability and effectiveness of the proposed algorithm in the MIMO antenna well.

In Fig. 5, the measured two-dimensional radiation patterns for optimized antenna at 5.5 GHz are presented, and only one antenna is excited for each measurement. Strong radiations have been

Figure 2. The Optimized Antenna Structure
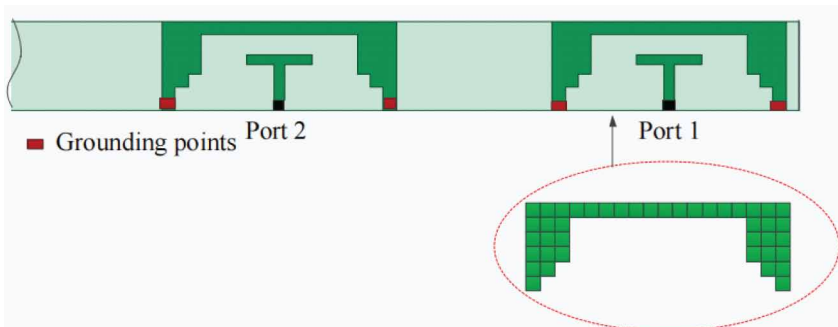
Figure 3. Simulated and Measured S-Parameter
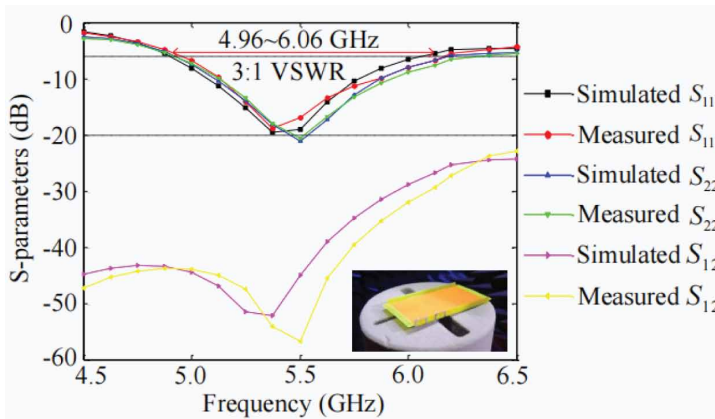
Figure 4. Advancing Trails of Some Representative Stars of Antenna Optimization by MOEA/D-BH
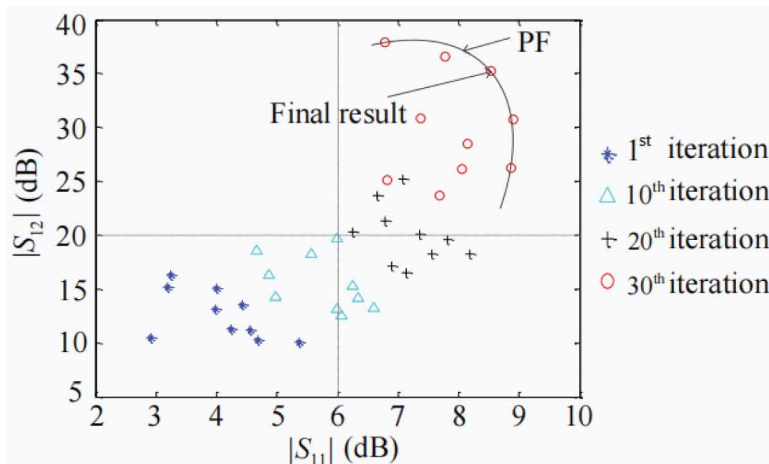
yielded in phi = 60° and phi = −60° directions for Antennas 1 and 2, respectively, thus resulting in good radiation diversity for complex scattering environments.

The simulated current distributions are shown in Fig. 6, where Antennas 1 and 2 are each excited at 5.5 GHz. When an antenna is excited, it can be observed that strong current is confined to its own area. This result explains why its isolation can be greater than 20 dB.

The measured total efficiency of MIMO antenna elements in LTE Band 46 is shown in Fig. 7. In the process of measurement, those factors that affect the efficiency are considered. Only one antenna element is excited for every measurement. As shown in Fig. 7, the total efficiency for LTE Band 46 varies from 69% to 79%. This can fully meet the actual needs for mobile applications.

Good envelope correlation coefficient (ECC) values can be seen from the above results in Fig. 5. The ECCs in LTE band 46 were then studied and are shown in Fig. 8. The ECCs are calculated by means of the formula in Sharawi (2013). Those results in the whole working band are far behind the acceptable criterion of ECC. In fact, lower ECCs are always along with higher diversity gain. Thus, the optimized MIMO antenna keeps good diversity performance.

Figure 5. Measured Two-Dimensional Radiation Patterns for Antennas 1 and 2 at 5.5 GHz
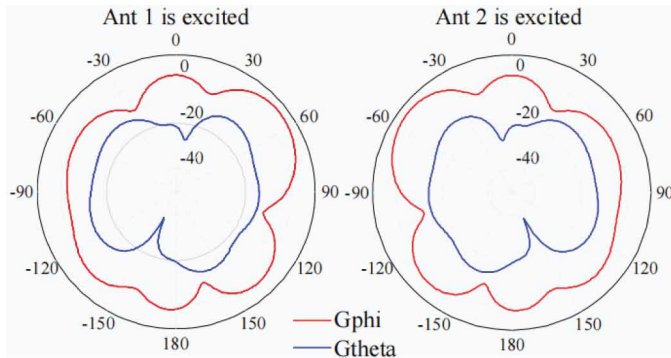
Figure 6. Simulated Current Distributions at 5.5 GHz
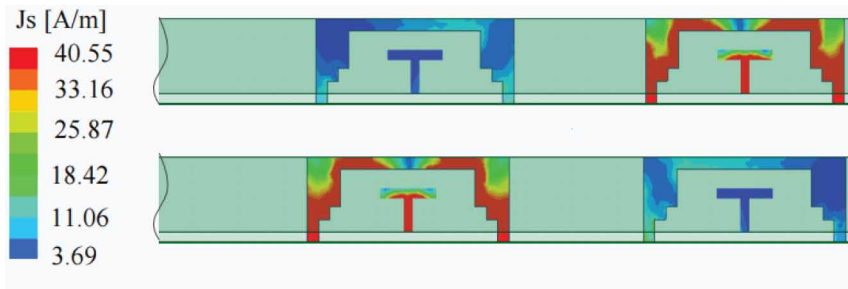
Further, similar algorithms MOEA/D-M (Li et al., 2020b) and MOEA/D-GO-II (Ding et al., 2017) and the original MOEA/D (Zhang & Li, 2007) are utilized to design the single-band antenna with the same initial conditions to prove the feasibility of MOEA/D-BH. In Fig. 9, the convergences for different algorithms are depicted with four different curves. MOEA/D-BH can find ideal results at the fastest speed, which indicates better convergence for our work. Furthermore, in terms of population diversity, MOEA/D-BH can provide more ideal results.

The correctness and practicability of MOEA/D-BH is verified first in the design of the single-band antenna.

Dual-Band MIMO Antenna Design

A dual-band MIMO antenna with higher design complexity is then optimized to verify the performance of MOEA/D-BH further. The dotted box is carried on more detailed division for better design. 36×6 small elements are defined as optimization parameters, and each element is $0.5 \times 1 \ mm^2$. Its evaluation function can also be set as Formula (5), and it should cover LTE Bands 42/43 (3.4~3.6 GHz, 3.6~3.8 GHz) and LTE Band 46. After multiple iterations by MOEA/D-BH, one of the obtained antenna structures is presented in Fig. 10.

The optimized dual-band MIMO antenna was simulated and measured, and its corresponding S-parameters are exhibited in Fig. 11. In all of the operation bands (LTE Bands 42/43/46), it demonstrates good S-parameter performance. Additionally, the simulation and measurement data have good consistency. These results further verify that the optimization of MIMO antenna by MOEA/D-BH is feasible.

Figure 7. Measured Total Efficiency in LTE Band 46
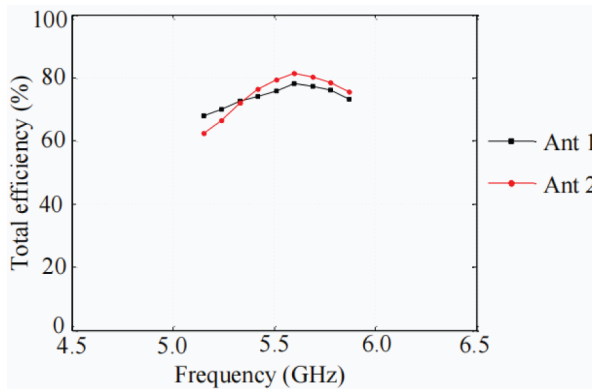
Figure 8. Calculated ECCs in LTE Band 46
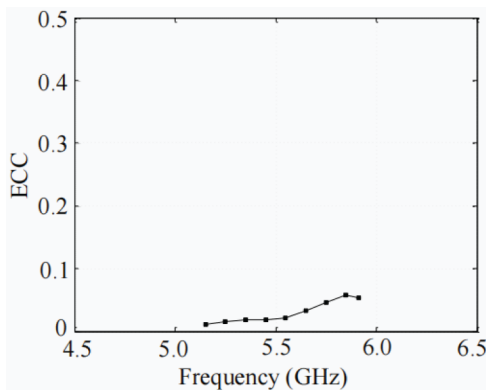
Figure 9. Comparison of Convergence Curves for Different Algorithms for Single-Band Antenna Design
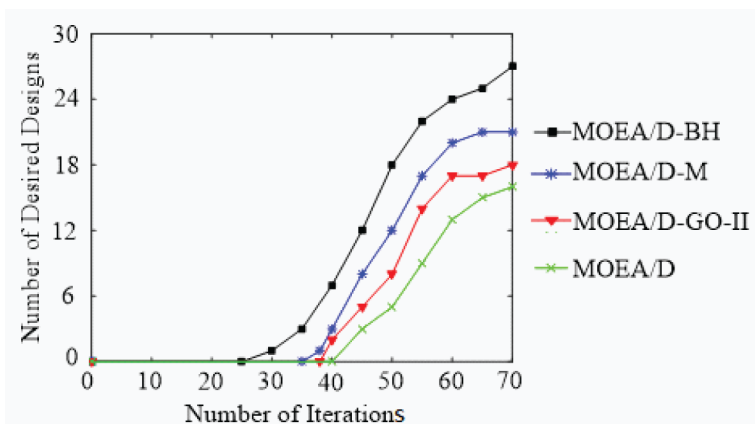
Figure 10. The Optimized Antenna Structure
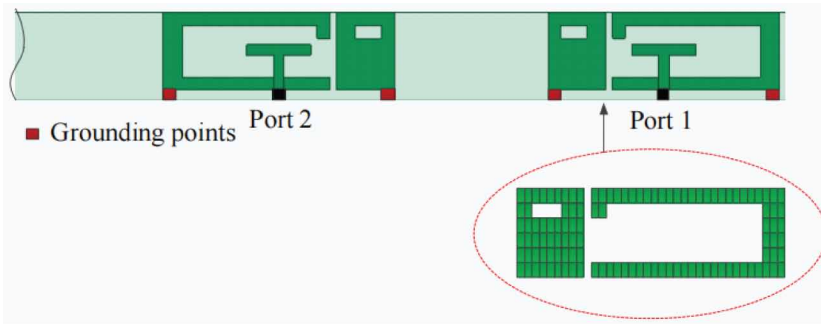
Figure 11. Simulated and Measured S-Parameters
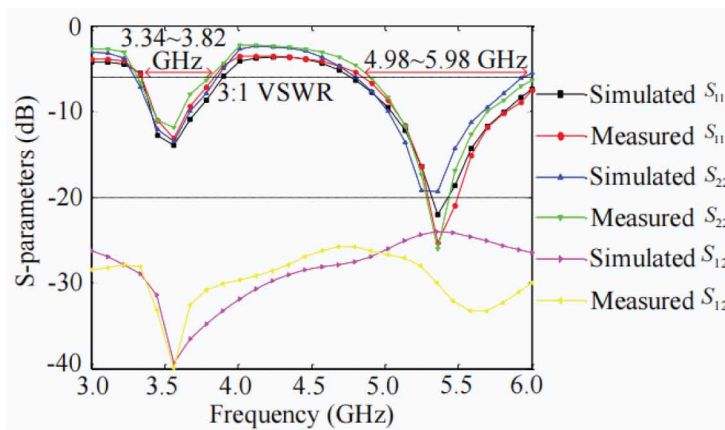
For Antennas 1 and 2, their measured two-dimensional radiation patterns at 3.6 GHz and 5.5 GHz are depicted in Fig. 12, where just one port is excited for each measurement. Strong radiation is presented near phi = 90° and phi = −90° directions at 3.6 GHz for Antennas 1 and 2, respectively, while phi = 60° and phi = −60° at 5.5 GHz. The antenna features good distinguishing and complementary patterns when the maximum radiation direction is scattered.

At 3.6 GHz and 5.5 GHz, the simulated current distributions for each antenna element are shown in Fig. 13. For every simulation, only one port is excited. From the figure, it can be seen that the right C-shape antenna contributes mainly to Band 3.6 GHz and the left rectangle antenna acts on 5.5 GHz. Current distributions also explain why the dual-band MIMO antenna can have satisfied isolation performance.

The measured total efficiency of MIMO antenna elements in LTE Band 46 is shown in Fig. 14. For LTE Bands 42/43, the total efficiency varies from 43% to 64%, and for LTE Band 46, it is from 60% to 79%. It is within a reasonable demand.

In Fig. 15, the calculated ECCs are presented, which can indicate the evaluation of diversity performance of the optimized MIMO antenna. In both working bands, the obtained ECCs are significantly greater than the available criterion, resulting in a good diversity capability of the optimized MIMO antenna.

Figure 12. Measured Two-Dimensional Radiation Patterns for Antennas 1 and 2 at 3.6 GHz (a, b) and at 5.5 GHz (c, d)
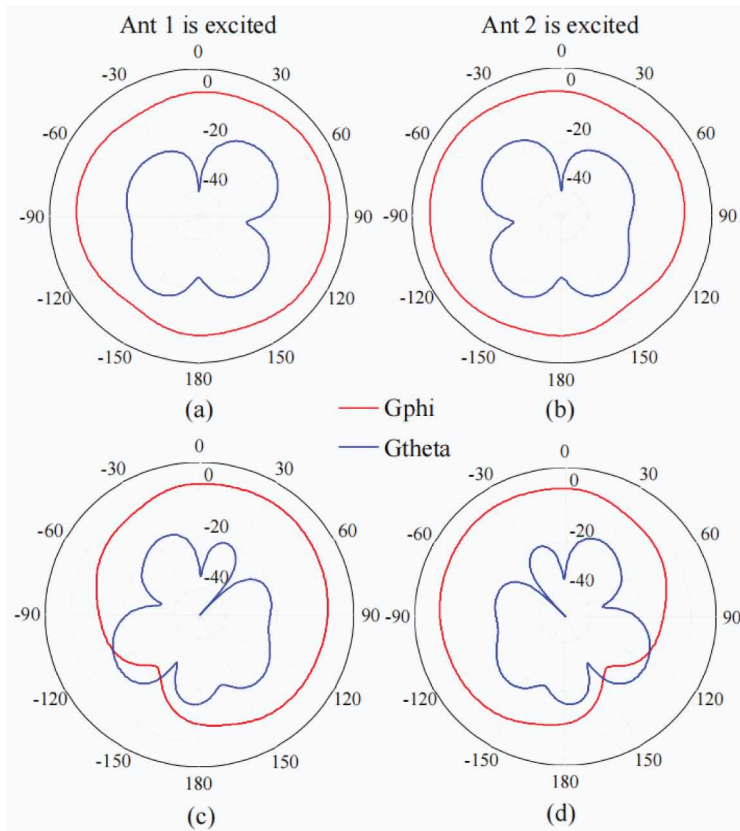
Figure 13. Simulated Current Distributions at 3.6 GHz (a, c) and at 5.5 GHz
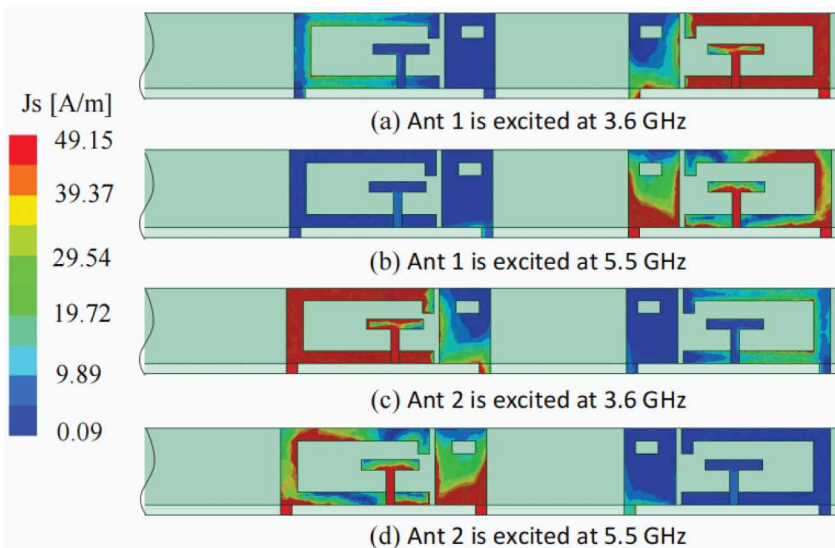
Figure 14. Measured Total Efficiency in LTE Bands 42/43/46
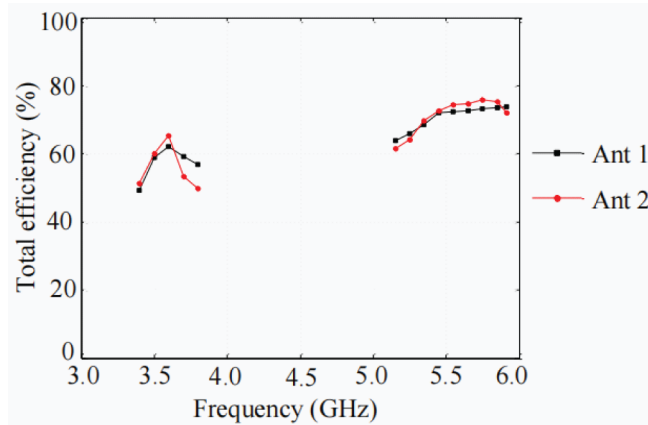
Figure 15. Calculated ECCs in LTE Bands 42/43/46
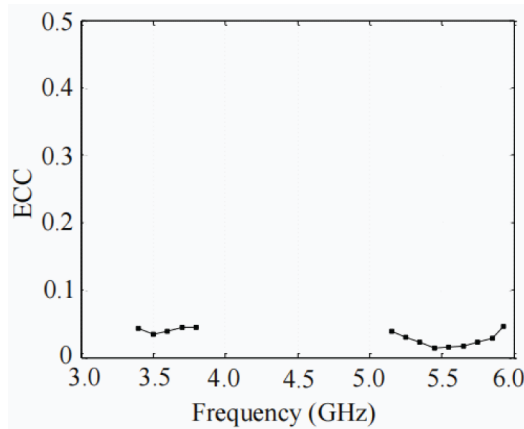
Eight-Port MIMO Antenna Design

The antenna element of the dual-band two-port MIMO antenna is used to make an eight-port MIMO antenna and fabricated for massive MIMO applications. Eight antenna elements are printed along the two edges of a FR-4 substrate, and every two antenna elements on one side are fixed as 20 mm here. The fabricated eight-port antenna is shown in Fig. 16.

Its simulated and measured S-parameters are given in Fig. 17. It can be observed that the S-parameter characteristics of Antennas 1 and 2 are in good agreement with the dual-band two-port MIMO antenna. The reflection coefficient of all antenna elements in LTE Bands 42/43/46 is lower than 6 dB, and the isolation of almost all antenna pairs (e.g., Antennas 1 and 4, Antennas 2 and 5) is better than 20 dB. An eight-port MIMO antenna can arguably work well in required bands with satisfied reflection coefficients and isolation performances. The measured total efficiency and calculated ECC values are presented in Fig. 18 and Fig. 19, respectively, and both perform well.

Using the formula presented in Tian et al. (2011), the ergodic channel capacities of the eight-port antenna were calculated. The propagation environment assumes that the transmitting antennas are uncorrelated and a Rayleigh fading channel is distributed independently and identically with a

Figure 16. Photo of the Fabricated Eight-Port Antenna
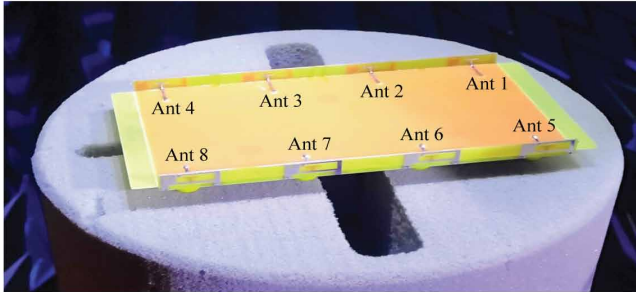
Figure 17. Simulated and Measured S-Parameters
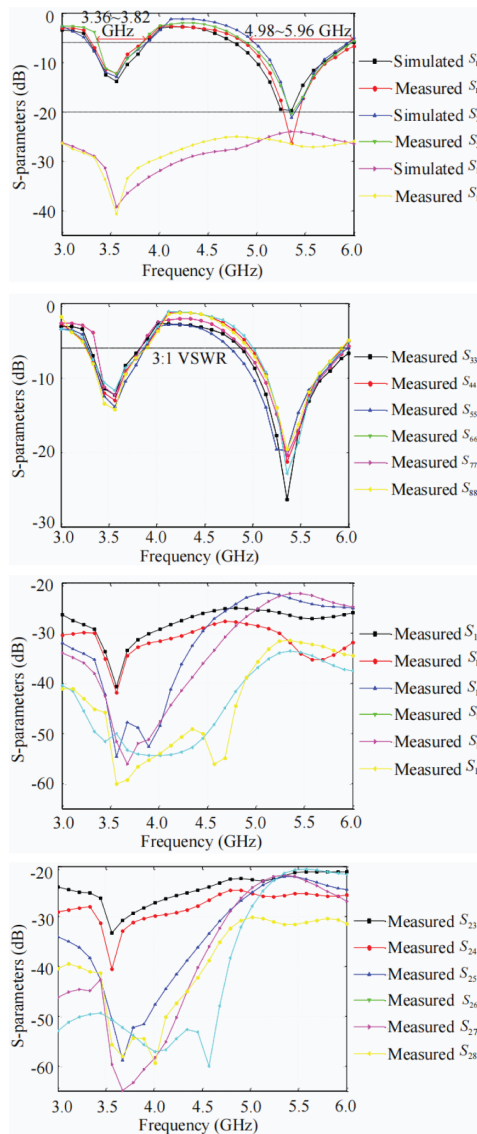
Figure 18. Measured Total Efficiency in LTE Bands 42/43/46
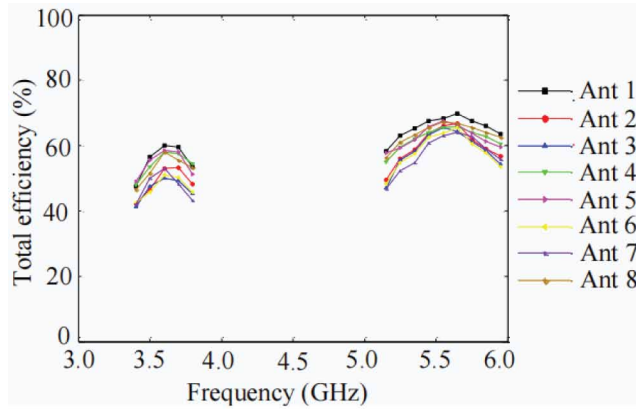
Figure 19. Calculated ECCs in LTE Bands 42/43/46
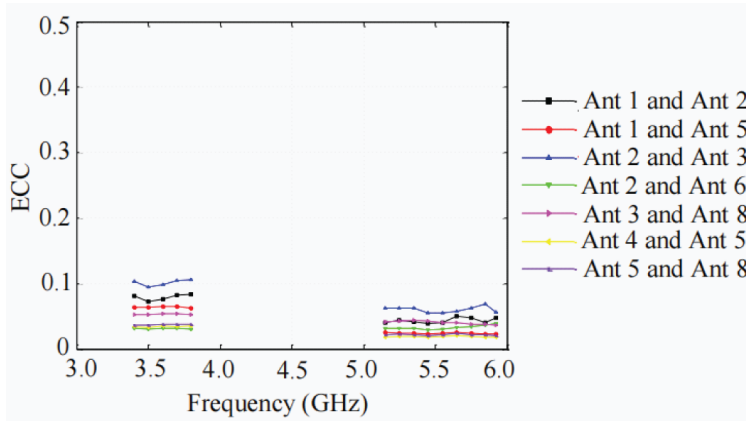
Figure 20. Calculated Ergodic Channel Capacity in LTE Bands 42/43/46
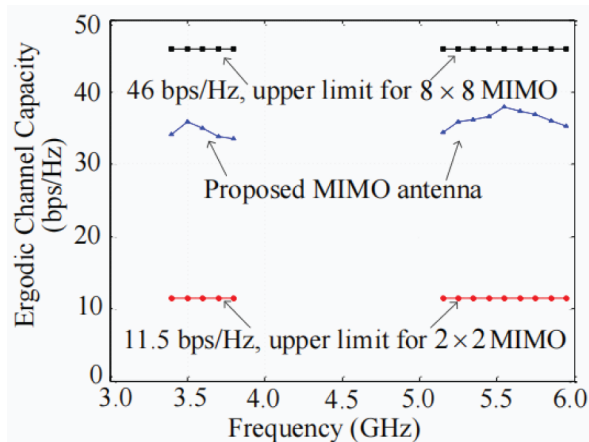
Table 1. Comparison of the Proposed Design and Those of Other Papers

Reference	Bandwidth (GHz)	Efficiency (%)	ECC	Maximum Channel Capacity (bps/Hz)
Wong et al. (2017)	3.4~3.6	40~52	< 0.15	35 (8×8, 20-dB SNR)
Zhao et al. (2019)	3.4~3.6	60~70	< 0.0125	37 (8×8, 20-dB SNR)
Proposed design	3.4~3.8 5.15~5.925	41~61 45~69	< 0.1 < 0.11	35 (2×8, 20-dB SNR) 38 (8×8, 20-dB SNR)

20-dB SNR (signal to noise ratio). Then, by averaging over 10,000 Rayleigh fading realizations, the ergodic channel capacities were obtained in all operation bands. As shown in Fig. 20, in LTE Bands 42/43 the maximum channel capacity is 35 bps/Hz and the minimum is 33 bps/Hz, while they are 38 bps/Hz and 34 bps/Hz in LTE Band 46. In comparison to the maximum capacity for 2×2 MIMO, it performs so much better. The quality of semantic communication can be ensured well.

The comparison of the proposed design and those of other papers reported for mobiles is shown in Table 1. Obviously, the proposed design can support wider useful bands, while the available bands of other papers are a little narrow. Meanwhile, the proposed design keeps comparable radiation and MIMO performances. Such a feature can be a unique strength for the proposed design and distinguish it from other reported designs.

The proposed scheme provides useful exploration for the development of intelligent semantic mobile systems. Thus, it is worth further research. The lack of reasonable correlation among the optimized discrete parameters in the design of antenna structures affects the optimization process greatly. Thus, it is very meaningful to study the correlation between optimization parameters based on a specific design problem. One major advantage of optimizing design is reducing time cost. However, due to the electromagnetic simulation for each antenna model during the optimization process, the optimization design scheme does not clearly demonstrate its advantage in time cost. Therefore, it is considered to introduce a surrogate model (e.g., a back-propagation neural network) to predict antenna performance. Then the applications of such schemes will be more extensive and convenient.

CONCLUSION

By introducing controllable absorption distance and a neighborhood learning mechanism, MOEA/D-BH presents good optimization performance for high-dimension parameters optimization of semantic-based mobile MIMO antennas. The design and analysis of two MIMO antennas prove this. Further, the performance of the eight-port MIMO antenna indicates its reliability in semantic-based mobile applications. In comparing to those previous similar designs, MOEA/D-BH can operate in wider bands without the weakening of electrical and MIMO performance. Depending weakly upon the initial model, our design of MIMO can provide a satisfactory antenna, and the final antenna is fabricated easily, although its shape is usually unexpected. It can be concluded that such a scheme is especially appropriate for new antenna design within an unexplored area. Moreover, for further studies on the MIMO antennas and other types of antenna design in a limited design space, it can also provide great new ideas. These schemes deserve further study.

CONFLICTS OF INTEREST

We wish to confirm that there are no known conflicts of interest associated with this publication and there has been no significant financial support for this work that could have influenced its outcome.

CORRESPONDING AUTHOR

Correspondence should be addressed to Qianqian Li (qqli_gdmec@163.com)

REFERENCES

Behera, T. K., Bakshi, S., Sa, P. K., Nappi, M., Castiglione, A., Vijayakumar, P., & Gupta, B. B. (2023). The NITRDrone dataset to address the challenges for road extraction from aerial images. *Journal of Signal Processing Systems for Signal, Image, and Video Technology*, *95*(2-3), 197–209. doi:10.1007/s11265-022-01777-0

Capuano, N., Foggia, P., Greco, L., & Ritrovato, P. (2022). A semantic framework supporting multilayer networks analysis for rare diseases. [IJSWIS]. *International Journal on Semantic Web and Information Systems*, *18*(1), 1–22. doi:10.4018/IJSWIS.297141

Ding, X. D., Ding, W. D., & Yang, L. X. (2017). *Modified MOEA/D-GO-II for design of fragment-type isolation structure between MIMO antennas*. NCMMW (2017).

Dong, J., Li, Q., & Deng, L. (2018). Design of fragment-type antenna structure using an improved BPSO. *IEEE Transactions on Antennas and Propagation*, *66*(2), 564–571. doi:10.1109/TAP.2017.2778763

Fatemidokht, H., Rafsanjani, M. K., Gupta, B. B., & Hsu, C. H. (2021). Efficient and secure routing protocol based on artificial intelligence algorithms with UAV-assisted for vehicular ad hoc networks in intelligent transportation systems. *IEEE Transactions on Intelligent Transportation Systems*, *22*(7), 4757–4769. doi:10.1109/TITS.2020.3041746

Geng, D., Li, H., & Liu, C. (2022). Tiny-UKSIE: An optimized lightweight semantic inference engine for reasoning uncertain knowledge. [IJSWIS]. *International Journal on Semantic Web and Information Systems*, *18*(1), 1–23. doi:10.4018/IJSWIS.300826

Han, J., Wang, G., & Sidén, J. (2015). Fragment-type UHF RFID tag embedded in QR barcode label. *Electronics Letters*, *51*(4), 313–315. doi:10.1049/el.2014.4355

Hatamlou, A. (2013). Black hole: A new heuristic optimization approach for data. *Information Sciences*, *222*, 175–184. doi:10.1016/j.ins.2012.08.023

Hu, B., Gaurav, A., Choi, C., & Almomani, A. (2022). Evaluation and comparative analysis of semantic web-based strategies for enhancing educational system development. [IJSWIS]. *International Journal on Semantic Web and Information Systems*, *18*(1), 1–14. doi:10.4018/IJSWIS.302895

Kaur, M., & Sivia, S. S. (2022). Artificial bee colony algorithm based modified circular-shaped compact hybrid fractal antenna for industrial, scientific, and medical band applications. *International Journal of RF and Microwave Computer-Aided Engineering*, *32*(3), e22994. doi:10.1002/mmce.22994

Li, H., & Zhang, Q. (2009). Multiobjective optimization problems with complicated Pareto sets, MOEA/D and NSGA-II. *IEEE Transactions on Evolutionary Computation*, *13*(2), 284–302. doi:10.1109/TEVC.2008.925798

Li, M., Tian, S., Tang, M. C., & Zhu, L. (2022). A compact low-profile hybrid-mode patch antenna with intrinsically combined self-decoupling and filtering properties. *IEEE Transactions on Antennas and Propagation*, *70*(2), 1511–1516. doi:10.1109/TAP.2021.3111638

Li, Q. Q., Chu, Q. X., & Chang, Y. L. (2020b). Design of compact high-isolation MIMO antenna with multiobjective mixed optimization algorithm. *IEEE Antennas and Wireless Propagation Letters*, *19*(8), 1306–1310. doi:10.1109/LAWP.2020.2997874

Li, Q. Q., Chu, Q. X., Chang, Y. L., & Dong, J. (2020a). Tri-objective compact log-periodic dipole array antenna design using MOEA/D-GPSO. *IEEE Transactions on Antennas and Propagation*, *68*(4), 2714–2723. doi:10.1109/TAP.2019.2949705

Lv, L., Wu, Z., Zhang, L., Gupta, B. B., & Tian, Z. (2022). An edge-AI based forecasting approach for improving smart microgrid efficiency. *IEEE Transactions on Industrial Informatics*, *18*(11), 7946–7954. doi:10.1109/TII.2022.3163137

Marler, R. T., & Arora, J. S. (2004). Survey of multi-objective optimization methods for engineering. *Structural and Multidisciplinary Optimization*, *26*(6), 369–395. doi:10.1007/s00158-003-0368-6

Miettinen, K. (1999). *Nonlinear multiobjective optimization*. Springer., doi:10.1007/978-1-4615-5563-6

Nhi, N. T. U., Le, T. M., & Van, T. T.Thanh The Van. (2022). A model of semantic-based image retrieval using C-tree and neighbor graph. [IJSWIS]. *International Journal on Semantic Web and Information Systems*, *18*(1), 1–23. doi:10.4018/IJSWIS.295551

Nouri, M., Abazari Aghdam, S., Jafarieh, A., Mallat, N. K., Haizal Jamaluddin, M., & Dor-Emami, M. (2021). An optimized small compact rectangular antenna with meta-material based on fast multi-objective optimization for 5G mobile communication. *Journal of Computational Electronics*, *20*(4), 1532–1540. doi:10.1007/s10825-021-01723-6

Rahman, M. A., Mukta, M. Y., Asyhari, A. T., Moustafa, N., Patwary, M. N., Yousef, A., Razzak, I., & Gupta, B. B. (2022). Renewable energy re-distribution via multiscale IoT for 6G-oriented green highway management. *IEEE Transactions on Intelligent Transportation Systems*, *23*(12), 23771–23780. doi:10.1109/TITS.2022.3203208

Sharawi, M. S. (2013). Printed multi-band MIMO antenna systems and their performance metrics [wireless corner]. *IEEE Antennas & Propagation Magazine*, *55*(5), 218–232. doi:10.1109/MAP.2013.6735522

Singh, S. K., Gupta, S., Kumar, S., Gupta, B. B., Alhalabi, V. A., & Zhang, J. (2024). A novel cumulative indicator score using indicator averaging for optimizing local business websites of enterprise systems. *Enterprise Information Systems*, *18*(2), 2301658. doi:10.1080/17517575.2023.2301658

Srivastava, D., Kumar, A., Mishra, A., Arya, V., Almomani, A., Hsu, C. H., & Santaniello, D. (2022). Performance optimization of multi-hop routing protocols with clustering-based hybrid networking architecture in mobile adhoc cloud networks. [IJCAC]. *International Journal of Cloud Applications and Computing*, *12*(1), 1–15. doi:10.4018/IJCAC.309932

Tian, R., Lau, B. K., & Ying, Z. (2011). Multiplexing efficiency of MIMO antennas. *IEEE Antennas and Wireless Propagation Letters*, *10*, 183–186. doi:10.1109/LAWP.2011.2125773

Wang, S., & Du, Z. (2015). Decoupled dual-antenna system using crossed neutralization lines for LTE/WWAN smartphone applications. *IEEE Antennas and Wireless Propagation Letters*, *14*, 523–526. doi:10.1109/LAWP.2014.2371020

Wen, L. H., Gao, S., Luo, Q., Mao, C. X., Hu, W., Yin, Y., Zhou, Y., & Wang, Q. (2018). Compact dual-polarized shared-dipole antennas for base station applications. *IEEE Transactions on Antennas and Propagation*, *66*(12), 6826–6834. doi:10.1109/TAP.2018.2871717

Wong, K. L., Tsai, C. Y., & Lu, J. Y. (2017). Two asymmetrically mirrored gap-coupled loop antennas as a compact building block for eight-antenna MIMO array in the future smartphone. *IEEE Transactions on Antennas and Propagation*, *65*(4), 1765–1778. doi:10.1109/TAP.2017.2670534

Zhang, Q., & Li, H. (2007). MOEA/D: A multiobjective evolutionary algorithm based on decomposition. *IEEE Transactions on Evolutionary Computation*, *11*(6), 712–731. doi:10.1109/TEVC.2007.892759

Zhang, S., Khan, S. N., & He, S. (2010). Reducing mutual coupling for an extremely closely-packed tunable dual-element PIFA array through a resonant slot antenna formed in-between. *IEEE Transactions on Antennas and Propagation*, *58*(8), 2771–2776. doi:10.1109/TAP.2010.2050432

Zhao, A., & Ren, Z. (2019). Size reduction of self-isolated MIMO antenna system for 5G mobile phone applications. *IEEE Antennas and Wireless Propagation Letters*, *18*(1), 152–156. doi:10.1109/LAWP.2018.2883428

Zou, X. J., Wang, G. M., Wang, Y. W., & Li, H. P. (2019). An efficient decoupling network between feeding points for multielement linear arrays. *IEEE Transactions on Antennas and Propagation*, *67*(5), 3101–3108. doi:10.1109/TAP.2019.2899039

Qian-Qian Li received the B.S. degree in communication engineering from the Hunan University of Science and Technology, Xiangtan, China, in 2015, the M.S. degree in information and communication engineering from Central South University, Changsha, China, in 2018, and Ph.D. degree in the School of Electronic and Information Engineering from South China University of Technology, Guangzhou, China in 2021. She works as a a lecturer at Guangdong Mechanical & Electrical Polytechnic. Her current research interests include intelligent optimization algorithms, array antennas and MIMO antennas.

Jian Dong received the B.S. degree in communication engineering at Hunan University in 2004, and the Ph.D. degree in information and communication engineering at the Huazhong University of Science and Technology (HUST) in 2010. He was a Research Assistant at National Key Laboratory of Science and Technology on Multispectral Information Processing of HUST from 2006 to 2010. He was a Visiting Scholar at the Eledia Research Center of University of Trento in Italy from 2016 to 2017. He works as a Full Professor at School of Electronic Information of Central South University. He published 6 books and over 150 peer-reviewed academic papers on international journals and conferences. He owns 23 innovation patents. His research interests include antennas, metamaterials, radars, machine learning and its applications to electromagnetics. He is the director of Hunan Engineering Research Center for new generation mobile communication RF inductive components. He is a member of Young Talents Board of Zhejiang Lab, a member of the expert database of the Ministry of Science and Technology, the National Natural Science Foundation, and the Ministry of Education. He has served as the guest Editor and Editorial Board member of some international journals, including Frontiers in Physics and Mathematics. He has served as a general co-chair of IoTCIT and 6GIoTT, as a technical program chair of CCPQT and EITCE, as a Session chair for IEEE ICMMT/IWS/NEMO/ISAPE/ISAP/IWAT, ACES, and PIERS.